Electronic Supplementary Material (ESI) for Journal of Materials Chemistry A.
This journal is © The Royal Society of Chemistry 2022

Supporting Information

Highly Efficient Bromine Capture and Storage Using N-Containing Porous Organic Cages

Sunggyu Lee[1,#], Ilia Kevlishvili[2,#], Heather J. Kulik[2], Hee-Tak Kim[1], Yongchul G. Chung[3*],
Dong-Yeun Koh[1,4*]

[1]Department of Chemical and Biomolecular Engineering (BK21 Four), Korea Advanced Institute of Science and Technology, Daejeon, 34141, South Korea

[2]Department of Chemical Engineering, Massachusetts Institute of Technology, Cambridge, Massachusetts 02139, United States

[3]School of Chemical Engineering, Pusan National University, Busan 46241, South Korea

[4]KAIST Institute for NanoCentury, Daejeon, 34141, South Korea

Detailed Synthetic Procedures of Porous Organic Cages (POCs)

Synthesis of CC3-R. Anhydrous Dichloromethane (20 ml) was layered slowly onto solid 1,3,5-triformylbenzene (TFB, 1 g, 6.17 mmol) without stirring at room temperature. Trifluoroacetic acid (TFA, 200 μL) was added directly to this solution as an acid-catalyst for the imine bond formation. Finally, a solution of (1R,2R)-cyclohexane-1,2-diamine (CHDA, 1 g, 8.76 mmol) in anhydrous dichloromethane (20 mL) was added to other solution without mixing. The reaction was covered and left to stand. Over 7 days, all of the solid TFB was used up and octahedral crystals of CC3-R grew on the sides of the glass reaction vessel. The crystalline product was collected by filtration and washed with mixture of EtOH/DCM (95:5, v/v).

Synthesis of FT-RCC3. Paraformaldehyde (52 mg, 20 eq.) dissolved in methanol (10 mL) was stirred at 70 °C. To this clear solution was added RCC3 (100 mg) dissolved in methanol (10 mL). A white precipitate appeared upon addition of RCC3. The reaction was stirred for a further 2 h at 70 °C. The reaction was cooled to room temperature and the precipitate was collected by filtration. FT-RCC3 (52 mg, 70 %) was obtained after being washed with methanol (3 × 10 mL) and dried under vacuum.

Adsorption Cyclic Performance

Experimental details. ~ 0.05g of CC3-R and ~ 0.3g of FT-RCC3 were used during sorption-desorption procedures. The adsorption procedure was performed during 24 hours under ambient, static conditions (25°C and 0.3 bar of Br_2 vapor pressure) and desorption procedure was performed during 24 hours at 200°C under dynamic vacuum condition. The bromine uptake capacity was meausred using the gravimetric method.

Density Functional Theory (DFT) calculations

Computational details. Geometry optimizations and frequency calculations were carried out using Orca 5.0.[1] All calculations were performed using the B3LYP[2] functional using Grimme's DFT-D4 dispersion correction,[3] and def2-SVP basis set in the gas phase. A tight SCF convergence threshold of 1 × 10^{-8} E_h was used for all calculations. Geometry optimizations were carried out using BFGS[4] in redundant internal coordinates implemented to the default tolerances of 3 × 10^{-4} hartree/bohr for the maximum gradient and 5 × 10^{-6} hartree for the change in energy between steps. Interaction energies between bromine clusters and POCs were further decomposed using the second generation energy decomposition analysis based on absolutely localized molecular orbitals (ALMO-EDA),[5] as implemented in Q-Chem 5.3.[6] Charge transfer interactions were further analyzed using the Complementary Occupied/Virtual Pairs (COVP) method.[7] Because the DFT-D4 dispersion correction is not implemented in Q-Chem, the decomposition was performed using B3LYP functional, and the dispersion interaction between two fragments was separately computed using the dftd4 conda package.[8]

Raman vibrational frequencies for Bromine molecules and cages are computed at the same level of theory. Since the chemical bonds are sensitive to the exchange-correlation functional, we benched marked several DFT functionals to compare with the experimental vibrational frequency of Br_2 and the results are tabulated in **Table S5**. For B3LYP functional, the Hartree-Fock exchange fractions of 25 and 30% were used to test the effect of varying degree of HFX on the vibrational frequency. The M06-2X functional with the def2-SVP basis set combination provided the best match between the simulation and experimental vibrational frequency for the Br_2 molecule but required 80% more time to run the calculations. In the interest of computational efficiency, we chose the B3YLP-D4 functional to compute the vibrational frequency of the cage and Br_2 molecules. Vibrational calculations were carried out numerically on the optimized geometry to compute the Hessian using the central difference approach as implemented in Orca 5.0. All vibrational frequency calculations are terminated until the SCF energy changes becomes less than 1.0 x 10^{-8} a.u. Each individual Raman line was modeled as homogeneously broadened Lorentzian function with a full half width of 20 cm^{-1}.

HBr formation. We calculated the reaction energies to form hydrobromic acid and bromide clusters with CC3-R and FT-RCC3 POCs, as well as model ligands forming these cages. These results are summarized in **Figure S30** and indicate significant stabilizing effect of POCs that can promote the formation of hydrobromic acid. While reactions are exergonic with CC3-R (ΔE = −2.3 and ΔE = −14.7 kcal/mol for the formation of Br_3^- and Br_5^-, respectively) and highly exergonic with FT-RCC3 (ΔE = −43.4 and ΔE = −52.0 kcal/mol), similar transformations using free ligands are highly endergonic.

Charge transfer analysis of POCs with bromine molecules. To better understand the difference in interactions between FT-RCC3 and CC3-R cages, we performed COVP analysis. The results from these calculations are summarized in **Figures S31** and **S32**. These calculations reveal that CC3-R cage can form highly stabilizing halogen bonding interactions with bromine, leading to 25.1 kcal/mol stabilization. Additionally, this complex is stabilized through $\pi \rightarrow \sigma^*_{Br\text{-}Br}$ and $n_{Br} \rightarrow \pi^*$ interactions (**Figure S31**). Similarly, FT-RCC3 is also stabilized through $n_N \rightarrow \sigma^*_{Br\text{-}Br}$ interactions, however, because tertiary amine groups are sterically not accessible, these interactions occur through hyperconjugation of amine lone pair to $\sigma^*_{C\text{-}H}$. Therefore, due to decreased overlap, overall charge transfer interactions are diminished between FT-RCC3 and three Br_2 molecules, with this primary interaction accounting only for 17.0 kcal/mol.

Grand Canonical Monte Carlo (GCMC) Simulations

Computational details. Grand Canonical Monte Carlo (GCMC) simulations were conducted to compute the maximum saturating loading of FT-RCC3 and CC3-R cages. CIF files for the structures were obtained from the literature, and the solvents were removed manually before the simulation. GCMC simulations were run at T = 298 K and P = 10 bar. Force field parameters for the cage were taken from the DREIDING force fields[9,] while the force field for bromine molecules was taken from Ref [10] (**Table S8**). Bromine is modeled as a two-center LJ model with zero partial atomic charges. The interatomic potentials to describe the interaction between the adsorbate and the framework atoms were approximated based on the Lennard-Jones 12-6 potential:

$$U_{ij} = 4\varepsilon_{ij}\left[\left(\frac{\sigma_{ij}}{r_{ij}}\right)^{12} - \left(\frac{\sigma_{ij}}{r_{ij}}\right)^{6}\right] \qquad \text{(S1)}$$

where U_{ij} is the interaction energy between atoms i and j, and r_{ij} is the center of the mass distance between the two atoms; ε_{ij} and σ_{ij} are the LJ parameters that correspond to the LJ potential well-depth and the van der Waals diameter, respectively. For the interaction between dissimilar atoms, the Lorentz-Berthelot mixing rules were used. The van der Waals interactions between atoms beyond the cutoff distance of 12.0 Å were not computed. Periodic boundary conditions were applied in xyz directions for the simulation.

GCMC simulations were carried out for 5,000 initialization cycles, followed by 10,000 production cycles, where 1 cycle is 20 or the number of molecules in the system, whichever number is greater. For each cycle, translation, reinsertion, and swap Monte Carlo moves were attempted with equal probabilities. Framework atoms were not allowed to change their positions during the GCMC simulations.

All simulations were carried out using the open-source RASPA software (v2.0.47)[11] compiled as a 64-bits application. Simulations were run on MacBookPro18,2 with ARM64 architecture. Random number seed of 1663849417 were used to generate the random number necessary for the selection of different Monte Carlo moves. Simulation snapshots were visualized using the iRASPA software[12].

128 **Figures S1-S34**

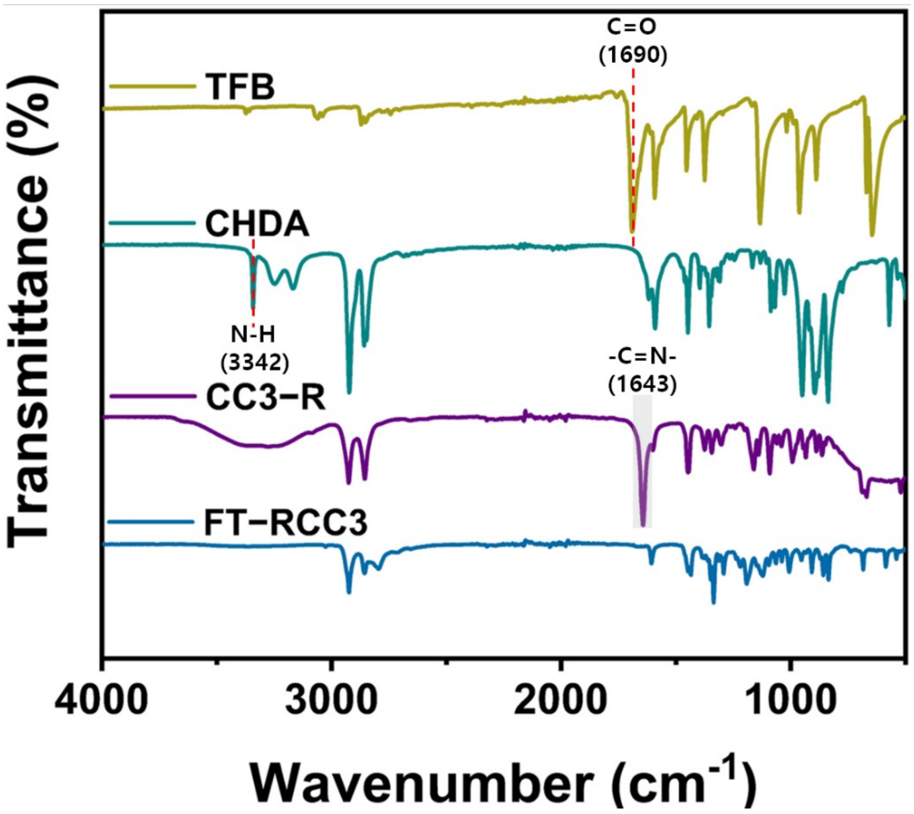

Figure S1. FT-IR spectra of monomers (TFB, CHDA) and POCs (CC3-R, FT-RCC3).

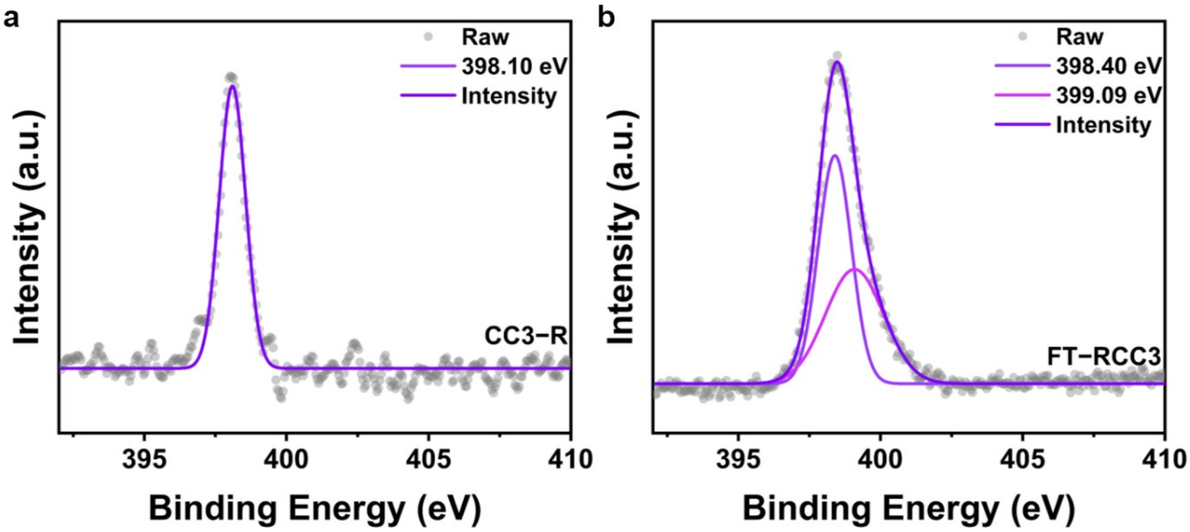

Figure S2. N_{1s} XPS spectra of (a) CC3-R and (b) FT-RCC3.

129

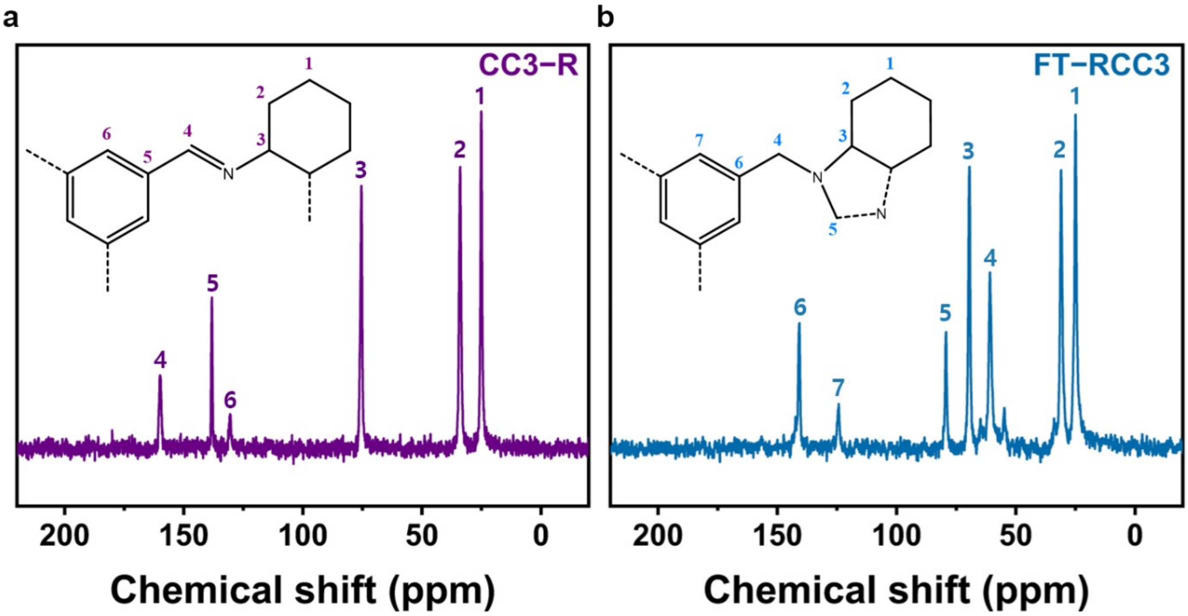

Figure S3. Solid-state ^{13}C CPMAS NMR spectra of (a) CC3-R and (b) FT-RCC3.

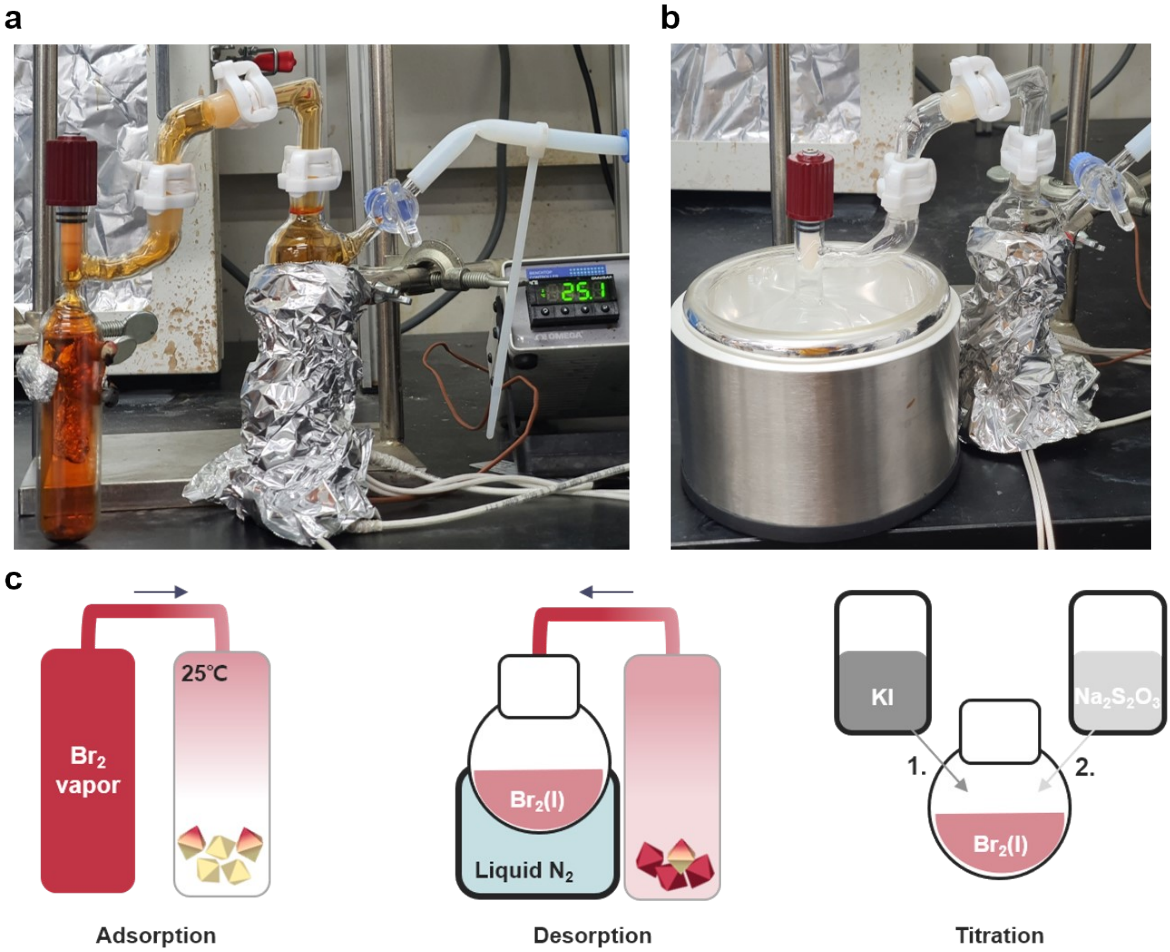

Figure S4. Photograph of Br_2 capture experiment during (a) adsorption and (b) desorption. (c) Schematic illustration of adsorption-desorption-titration procedure.

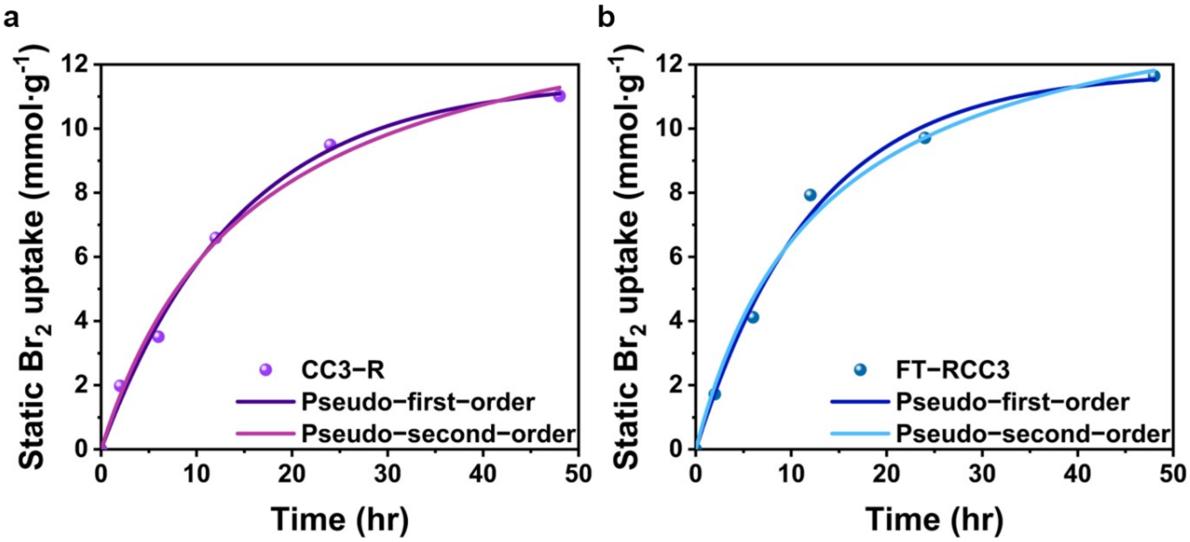

Figure S5. Adsorption kinetic curve of (a) CC3-R and (b) FT-RCC3. Graph were fitted using pseudo-first-order and pseudo-second-order adsorption model.

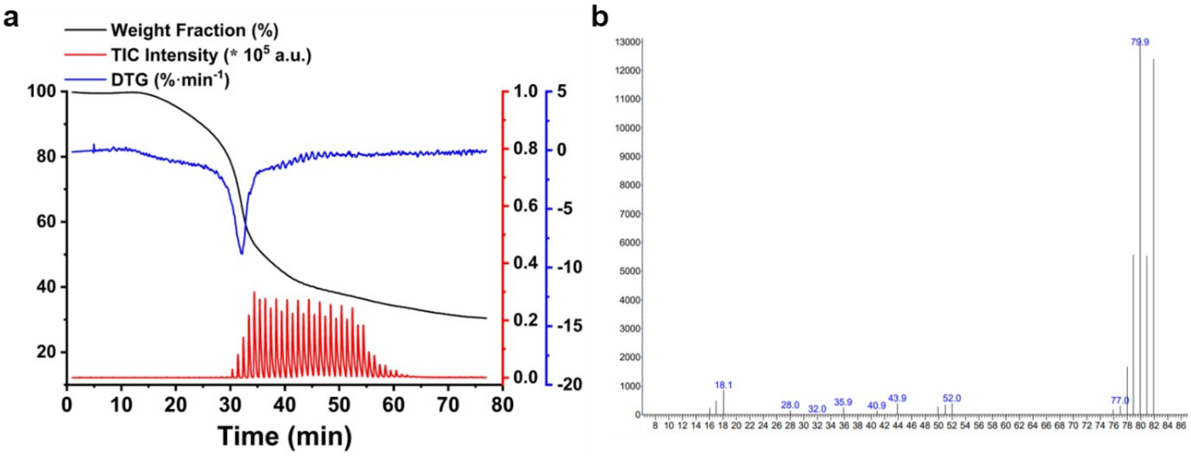

Figure S6. EGA profile of Br_2@CC3-R after thermal treatment. (a) TGA, DTG and TIC curve and (b) mass spectra of evolved gas.

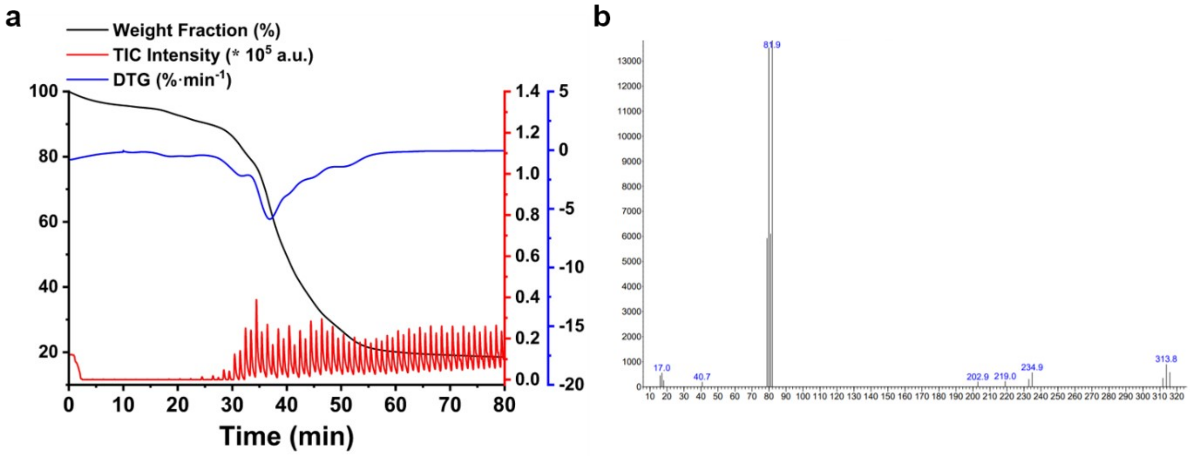

Figure S7. EGA profile of Br_2@FT-RCC3 after thermal treatment. (a) TGA, DTG and TIC curve and (b) mass spectra of evolved gas.

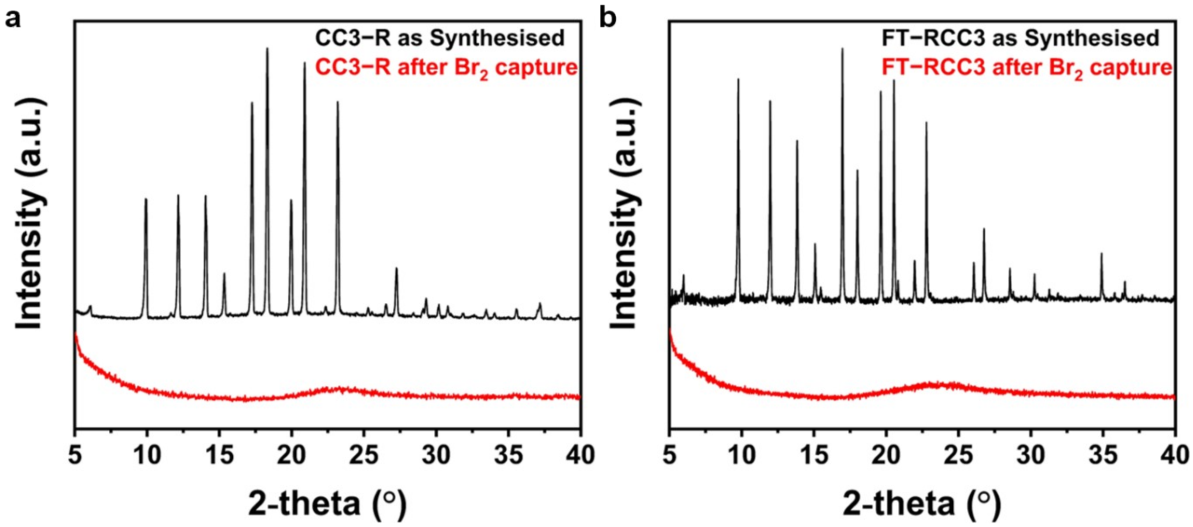

Figure S8. PXRD patterns of pristine and Br_2 captured (a) CC3-R and (b) FT-RCC3.

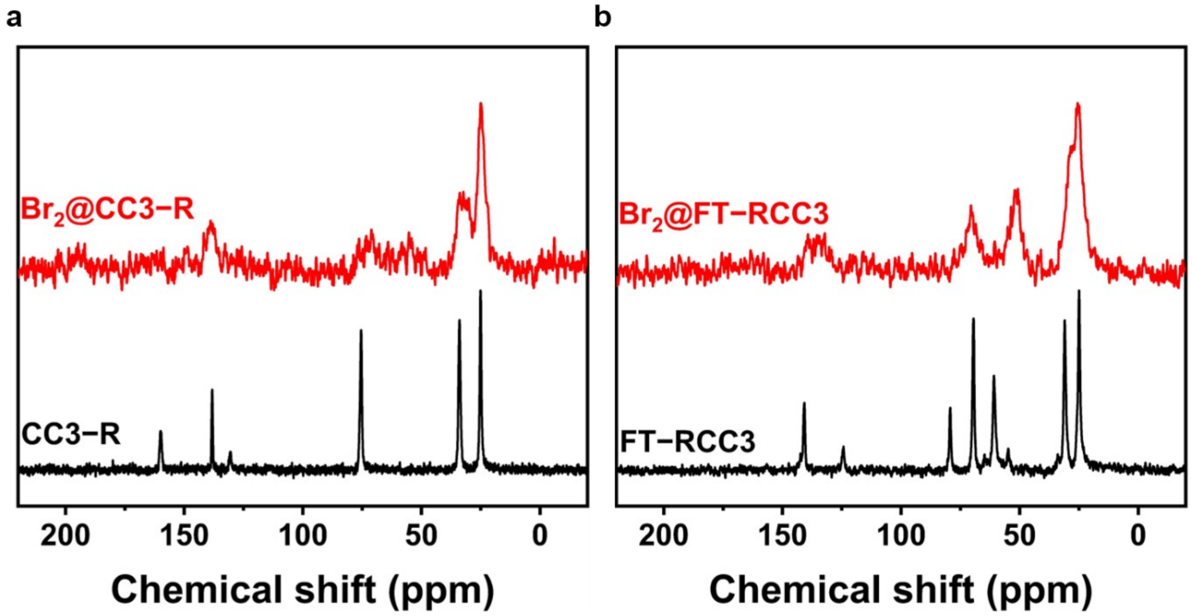

Figure S9. Solid-state ^{13}C CP MAS NMR spectra of pristine (black line) and Br_2 captured (red line) (a) CC3-R and (b) FT-RCC3.

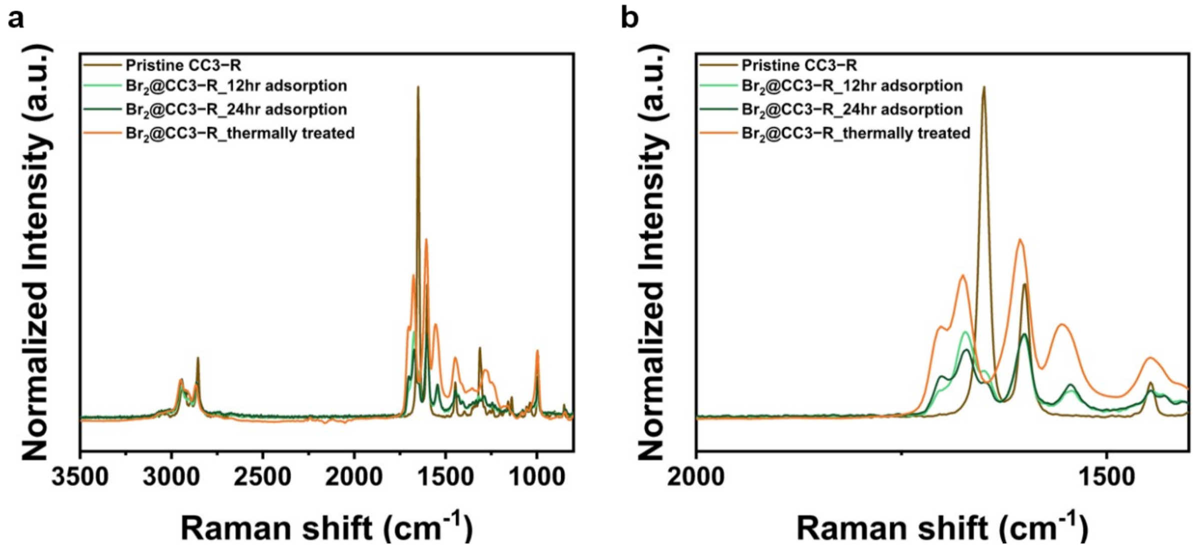

Figure S10. Raman spectra of pristine CC3-R, Br_2@CC3-R and thermally treated Br_2@CC3-R. (a) Full spectrum range and (b) 2000 cm^{-1} to 1400 cm^{-1} range.

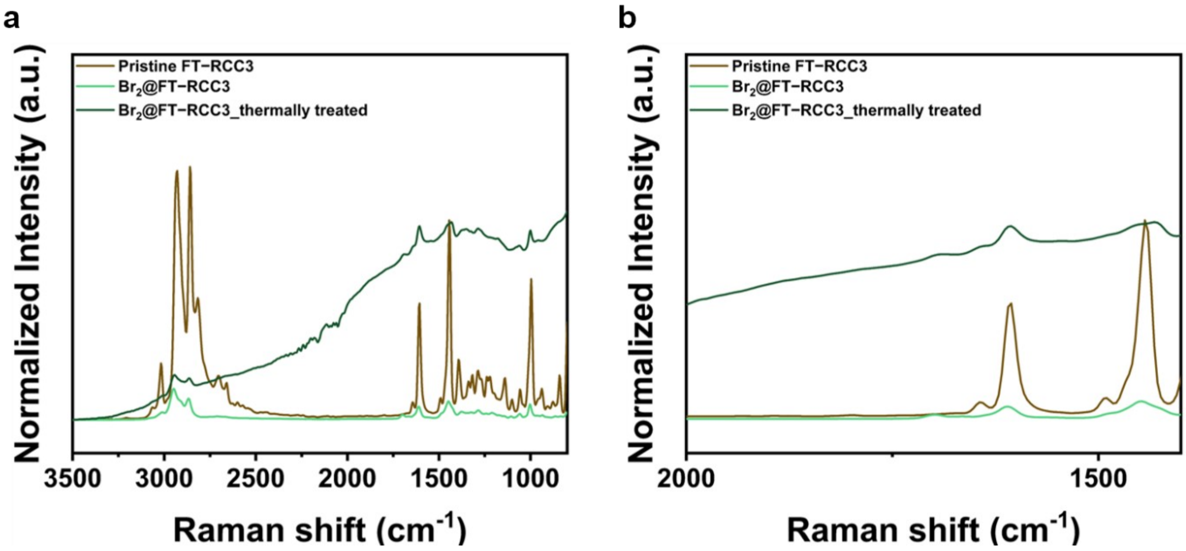

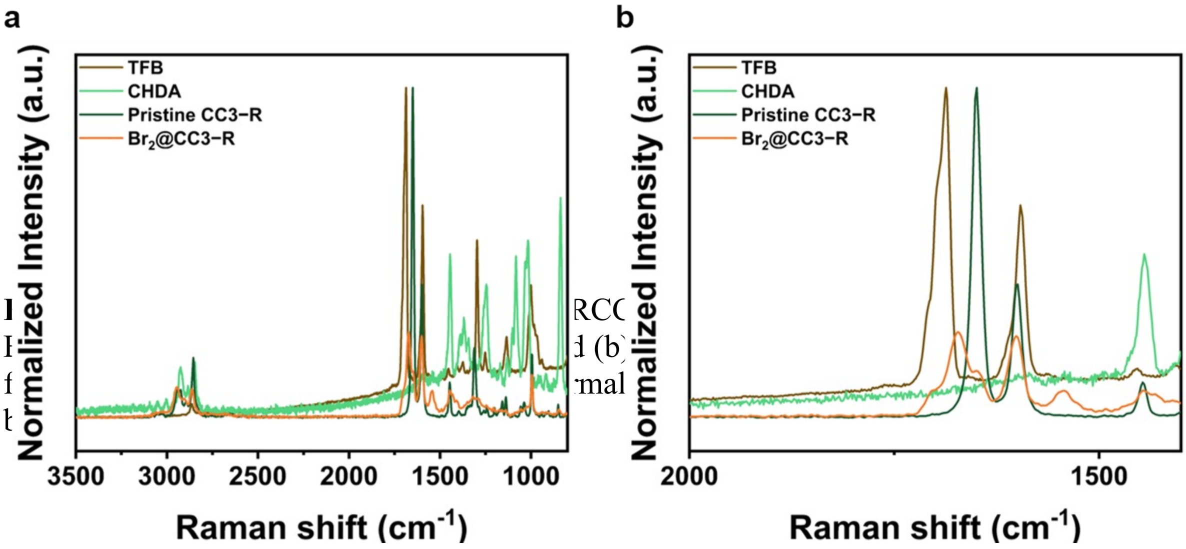

Figure S12. Raman spectra of monomers (TFB and CHDA), pristine CC3-R and Br_2@CC3-R. (a) Full spectrum range and (b) 2000 cm^{-1} to 1400 cm^{-1} range.

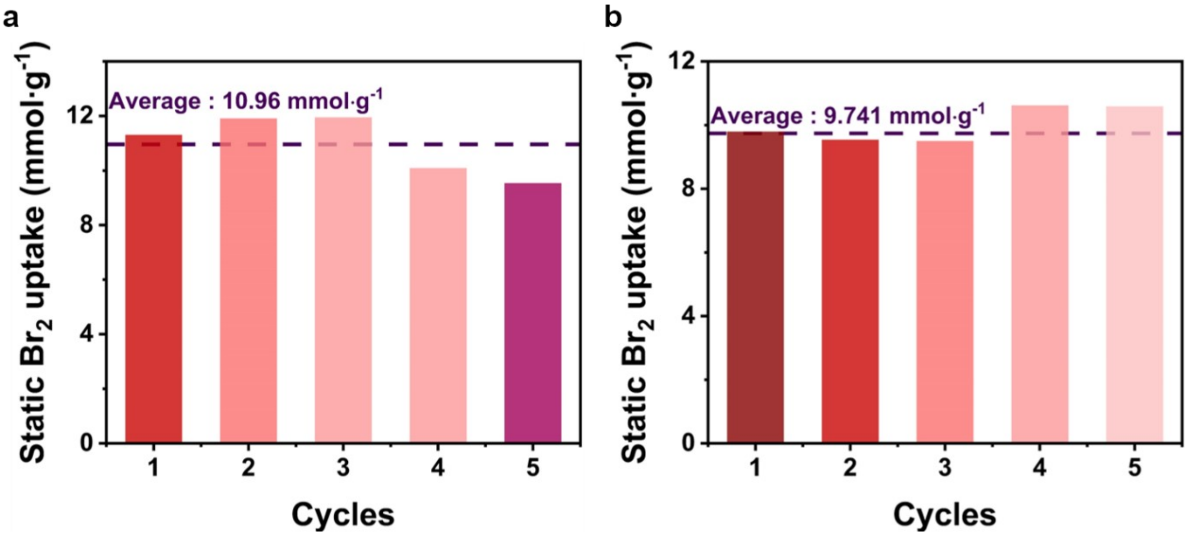

Figure S13. Adsorption cyclic capacities of (a) CC3-R and (b) FT-RCC3 over 5 consecutive cycles. In the case of (a) CC3-R, there were some deviations in the adsorption capacities compared to those of large scale CC3-R (~ 15% higher value than those of large scale CC3-R; 10.96 mmol/g_small scale vs 9.49 mmol/g_large scale)

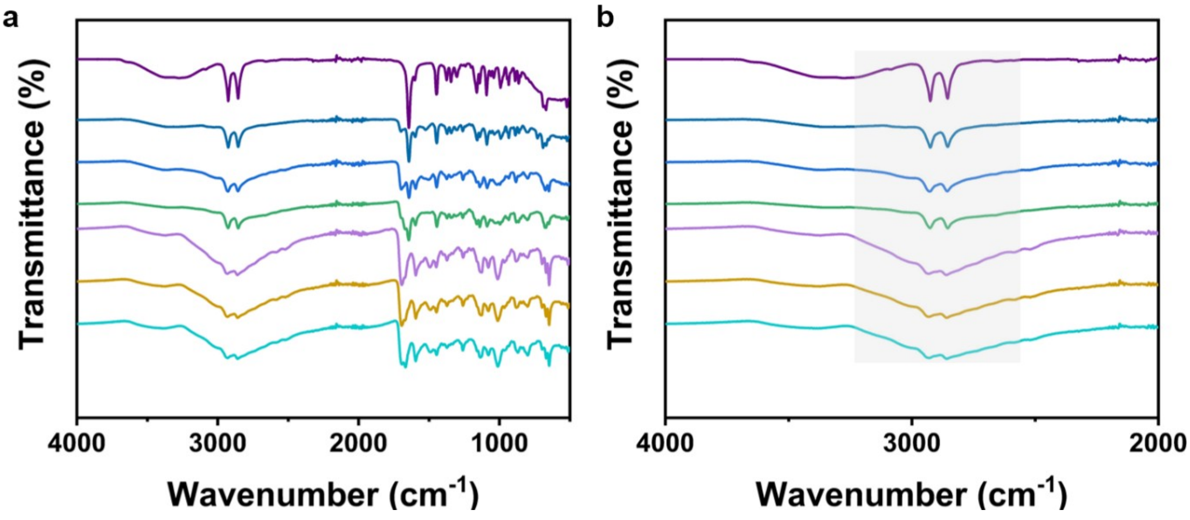

Figure S14. Time-resolved FT-IR spectra of CC3-R during Br_2 adsorption. (a) Full spectrum range and (b) 4000 cm^{-1} to 2000 cm^{-1} range.

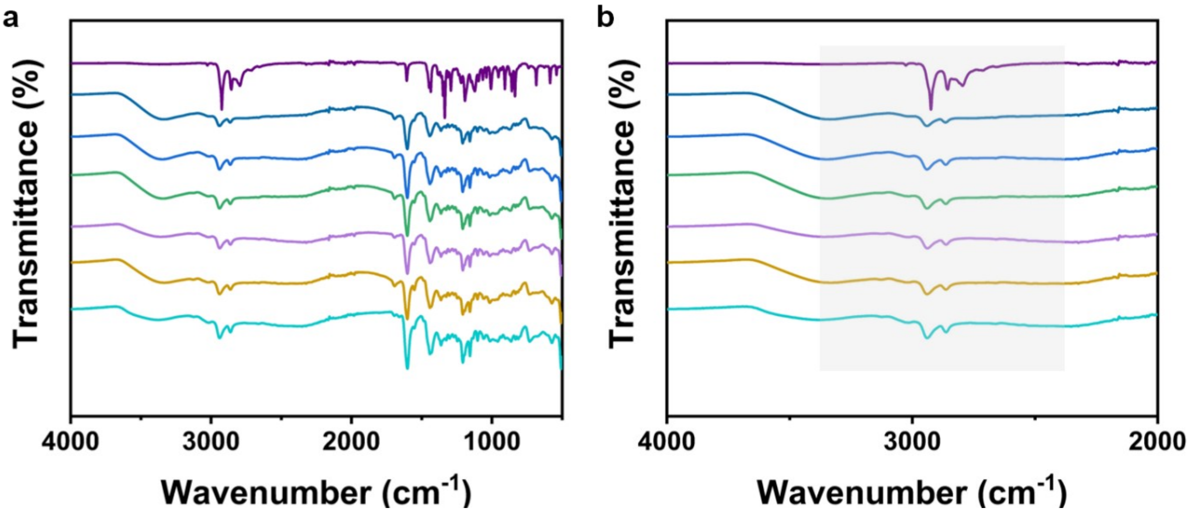

Figure S15. Time-resolved FT-IR spectra of FT-RCC3 during Br_2 adsorption. (a) Full spectrum range and (b) 4000 cm^{-1} to 2000 cm^{-1} range.

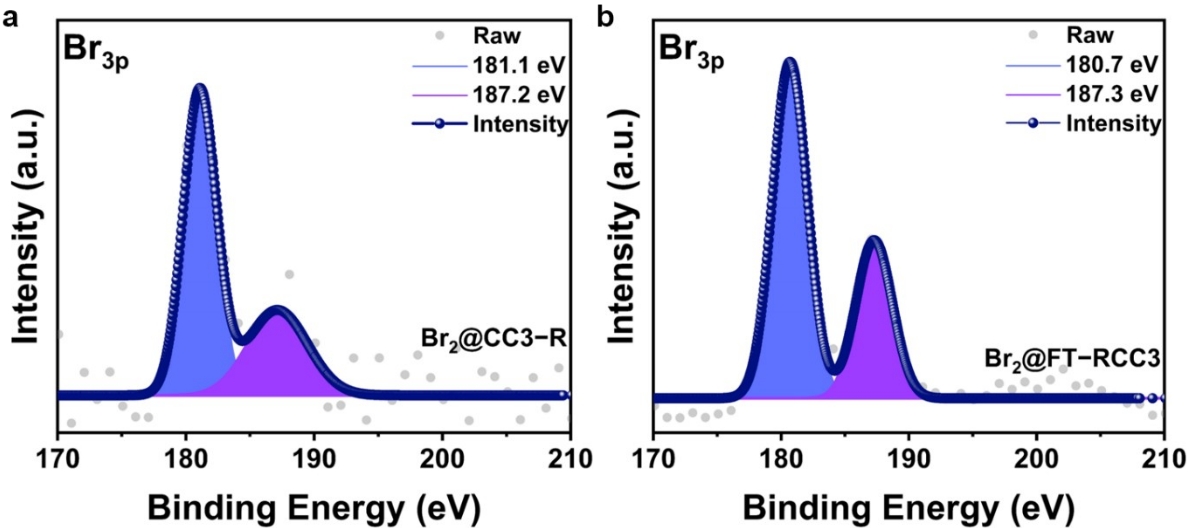

Figure S16. Br_{3p} XPS spectra of (a) Br_2@CC3-R and (b) Br_2@FT-RCC3.

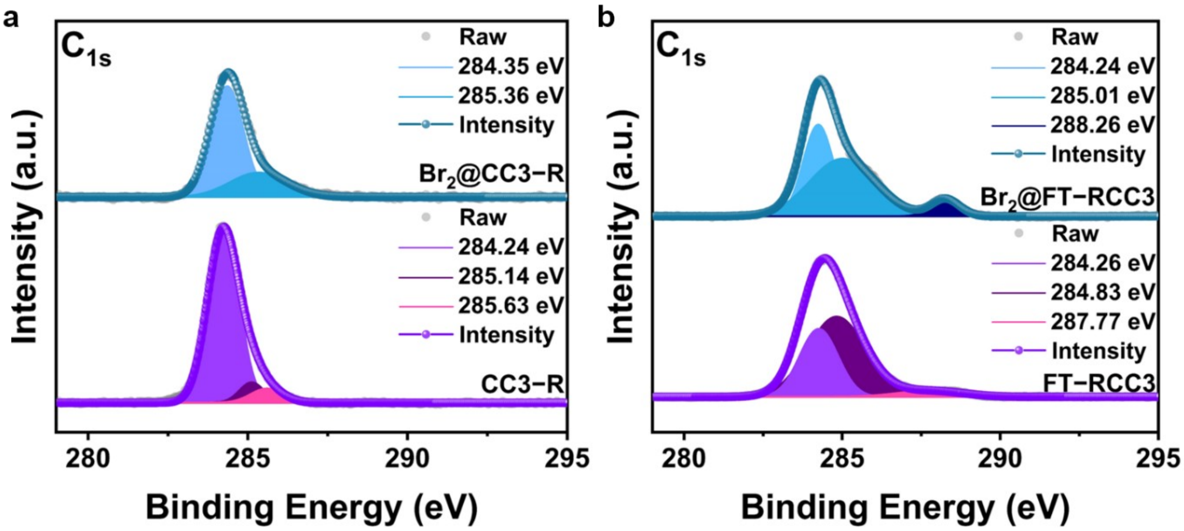

Figure S17. C_{1s} XPS spectra of (a) Br_2@CC3-R and (b) Br_2@FT-RCC3.

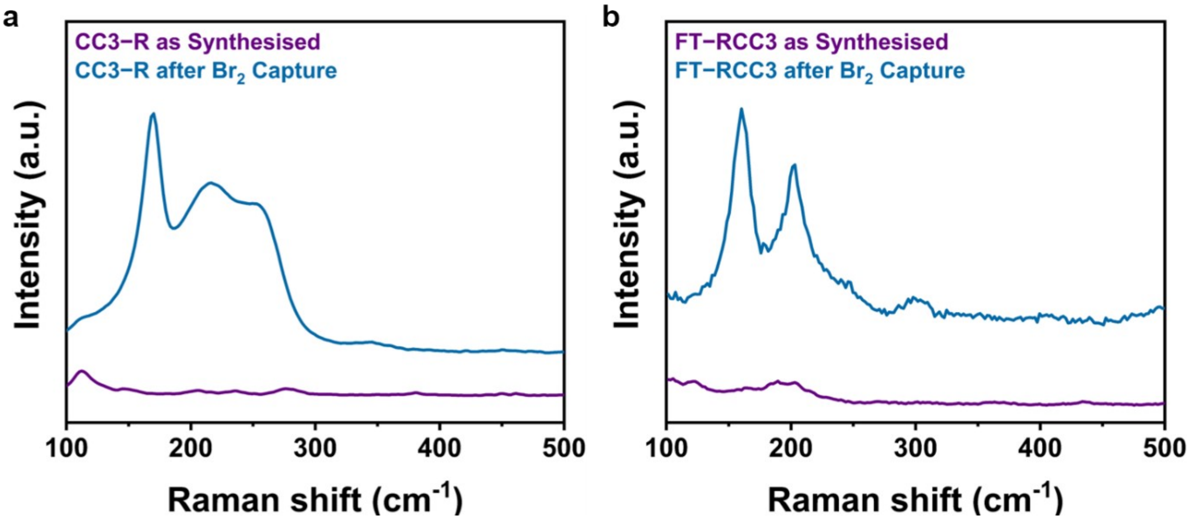

Figure S18. Raman spectra of pristine and Br_2 captured (a) CC3-R and (b) FT-RCC3.

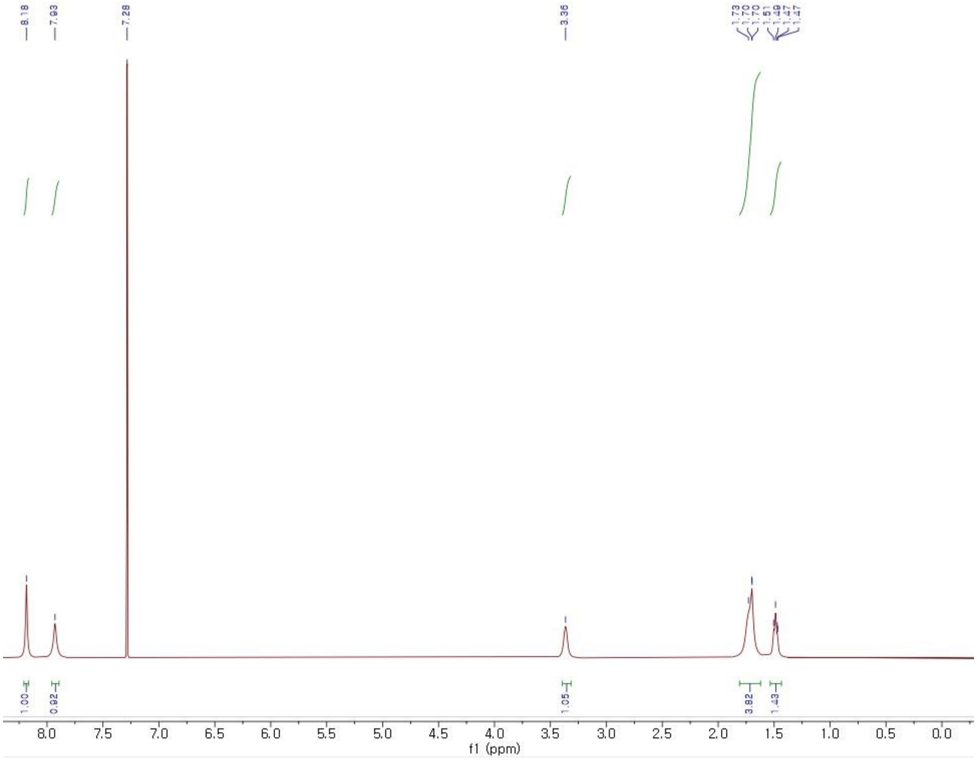

Figure S19. ^{1}H NMR of CC3-R in $CDCl_3$ at 25 °C.

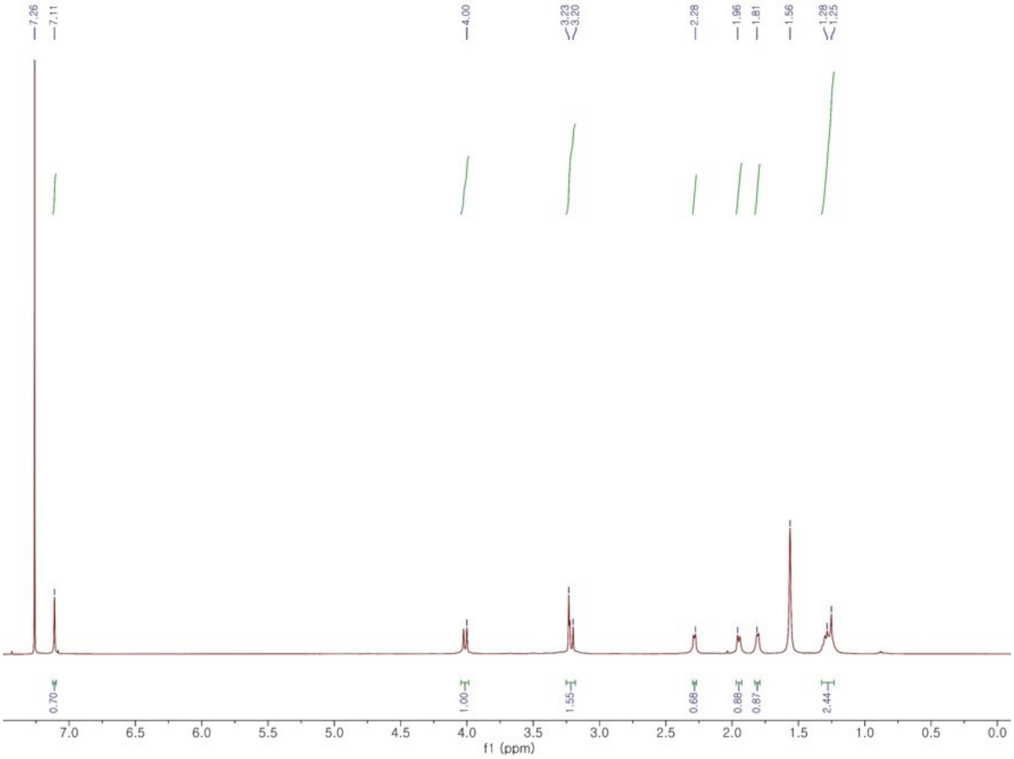

Figure S20. ^{1}H NMR of FT-RCC3 in $CDCl_3$ at 25 °C.

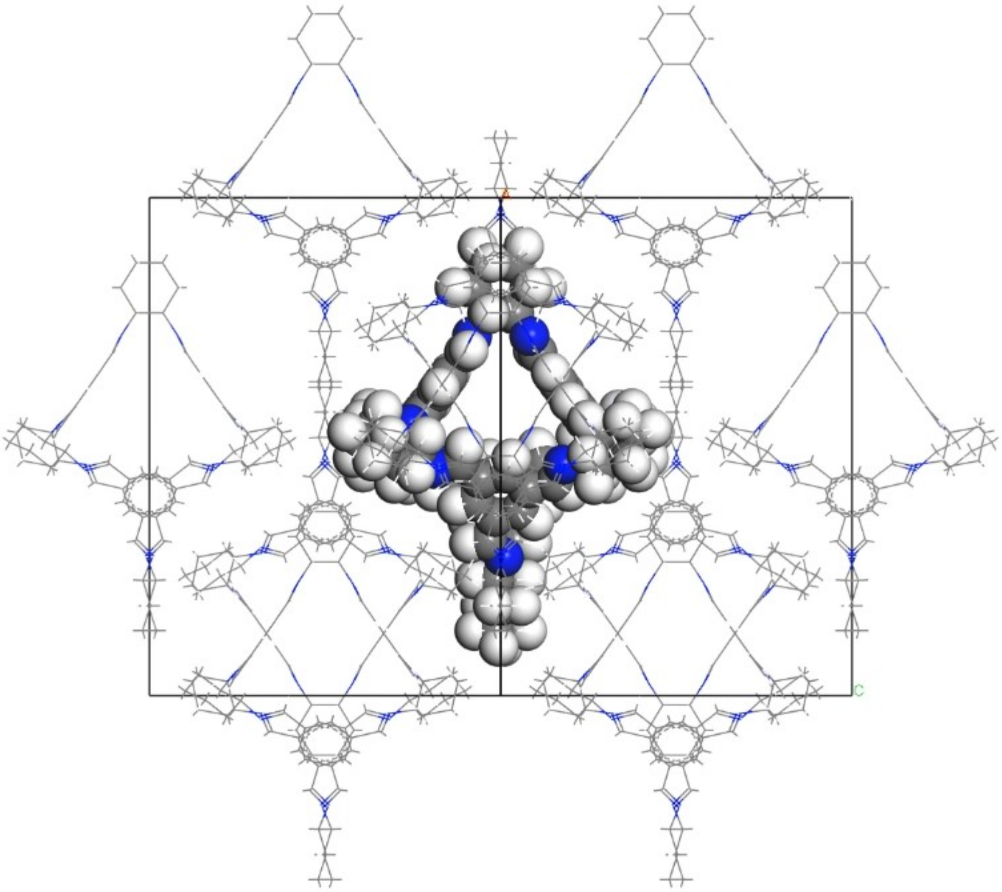

Figure S21. Packing of FT-RCC3 in a unit cell. Part of the unit cell that are used for the modeling is rendered in CPK.

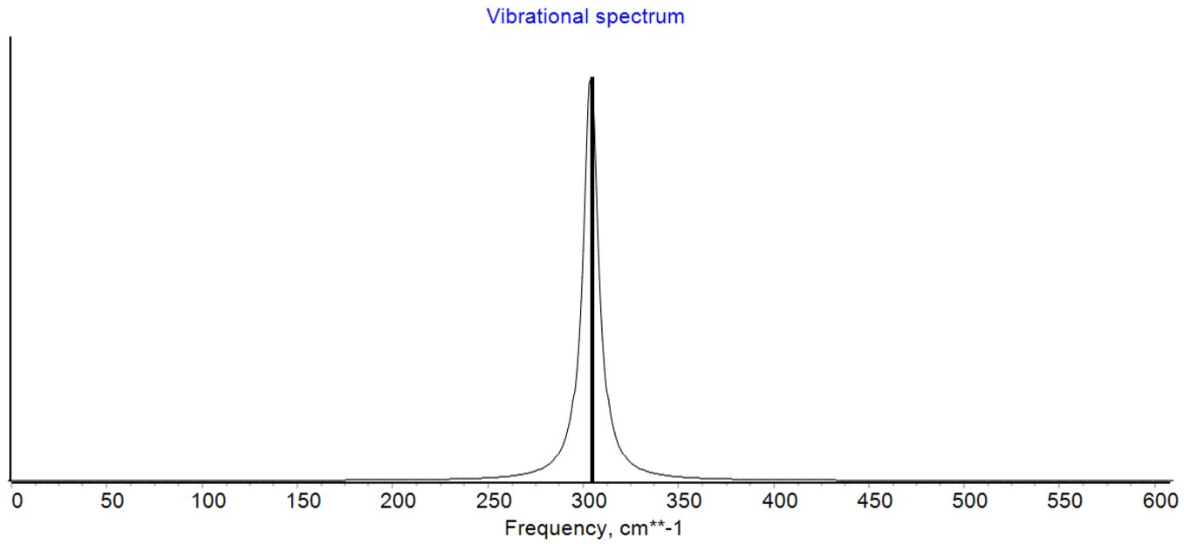

Figure S22. Calculated Raman vibrational spectrum of Br_2.

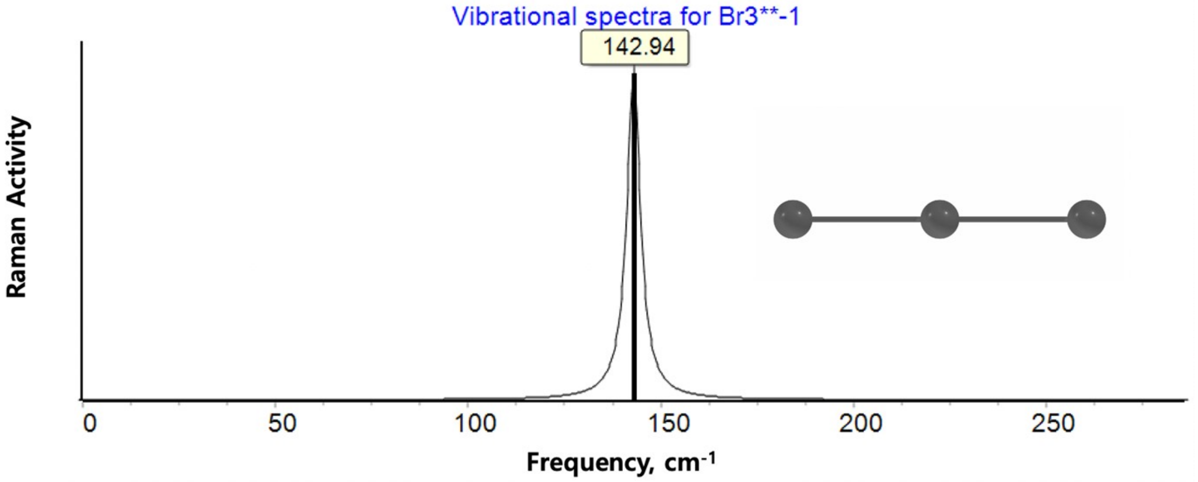

Figure S23. Calculated Raman vibrational spectrum of Br_3^-. The optimized geometry of Br_3^- is shown in the inset.

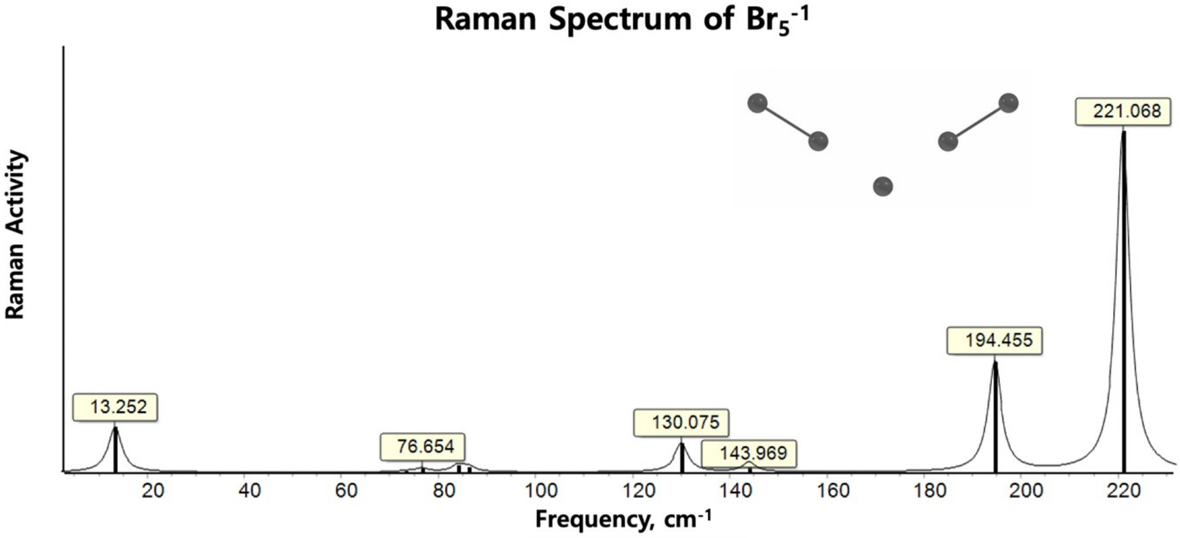

Figure S24. Calculated Raman vibrational spectrum of Br_5^-. Symmetric stretching is at 221 cm^{-1} while 194 cm^{-1} corresponds to the asymmetric stretching.

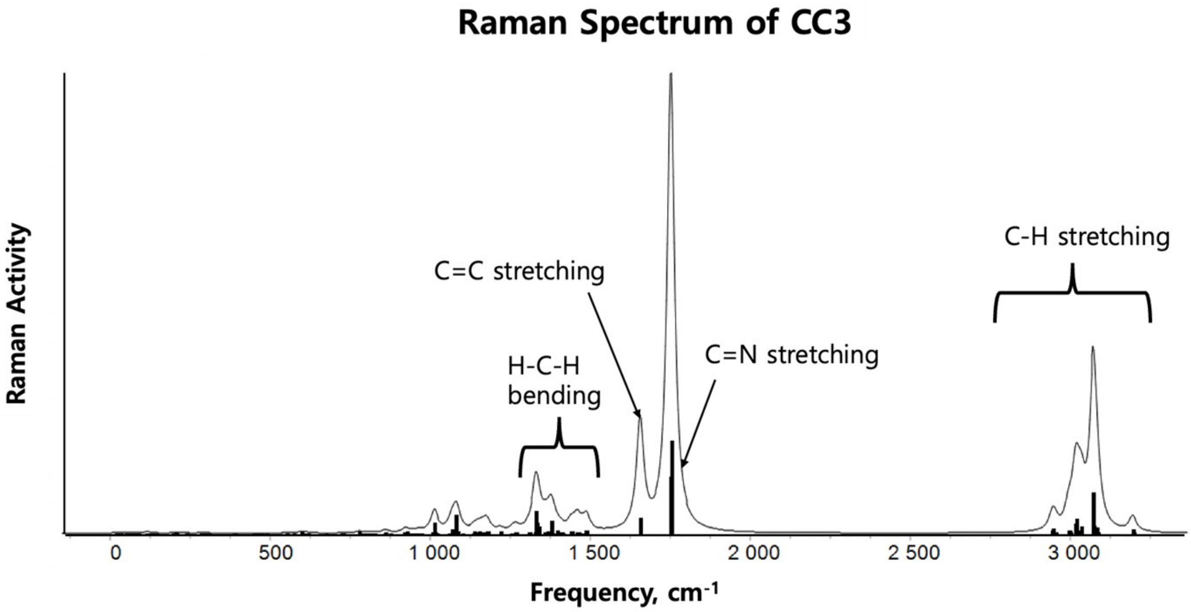

Figure S25. Calculated Raman vibrational spectrum of CC3.

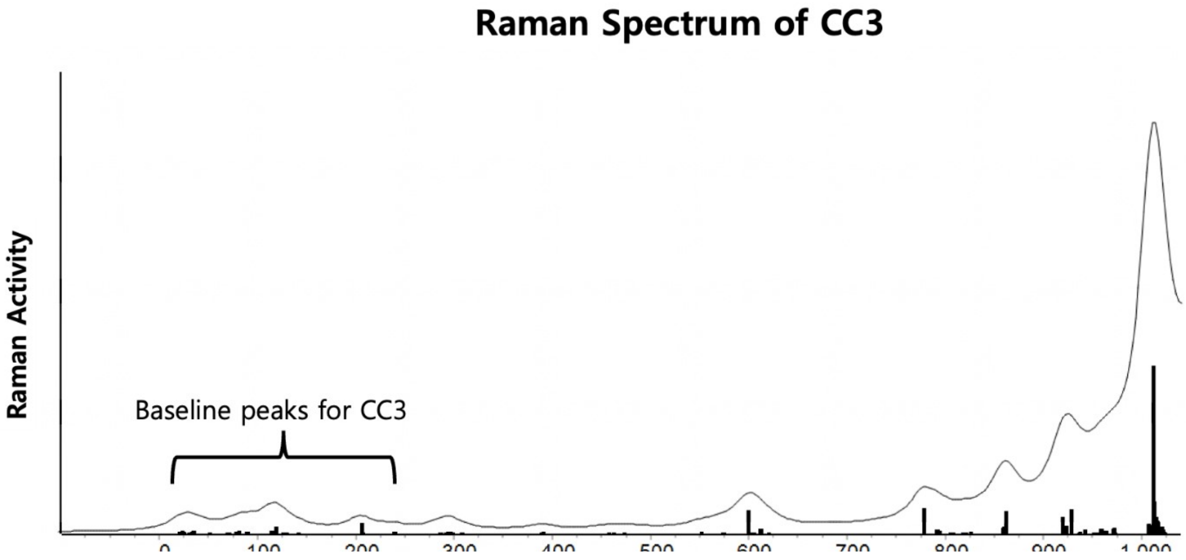

Figure S26. Calculated Raman vibrational spectrum of CC3 from 0 – 1000 cm^{-1}.

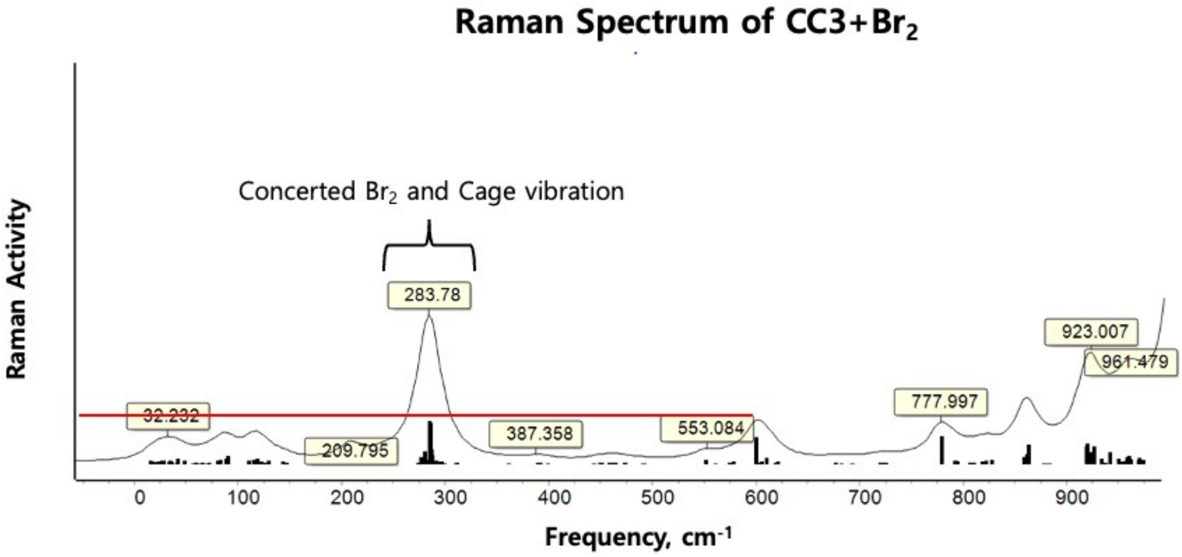

Figure S27. Calculated Raman vibrational spectrum of CC3 and adsorbed Br_2 molecule. The red line is the guide to the eyes.

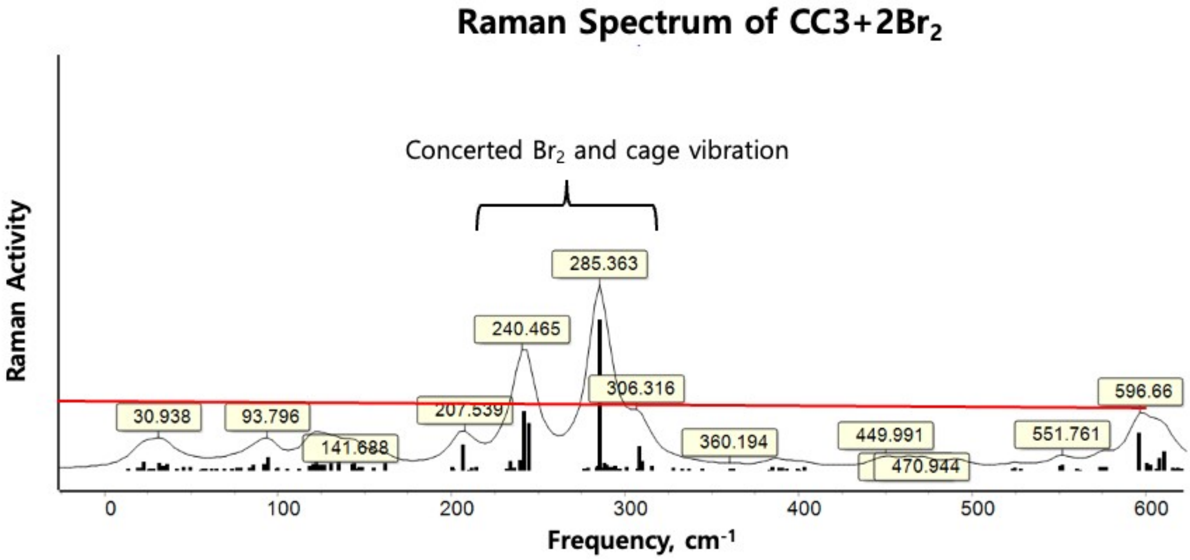

Figure S28. Calculated Raman vibrational spectrum of CC3 with adsorbed 2 molecules of Br_2 adsorbed. The red line is the guide to the eyes.

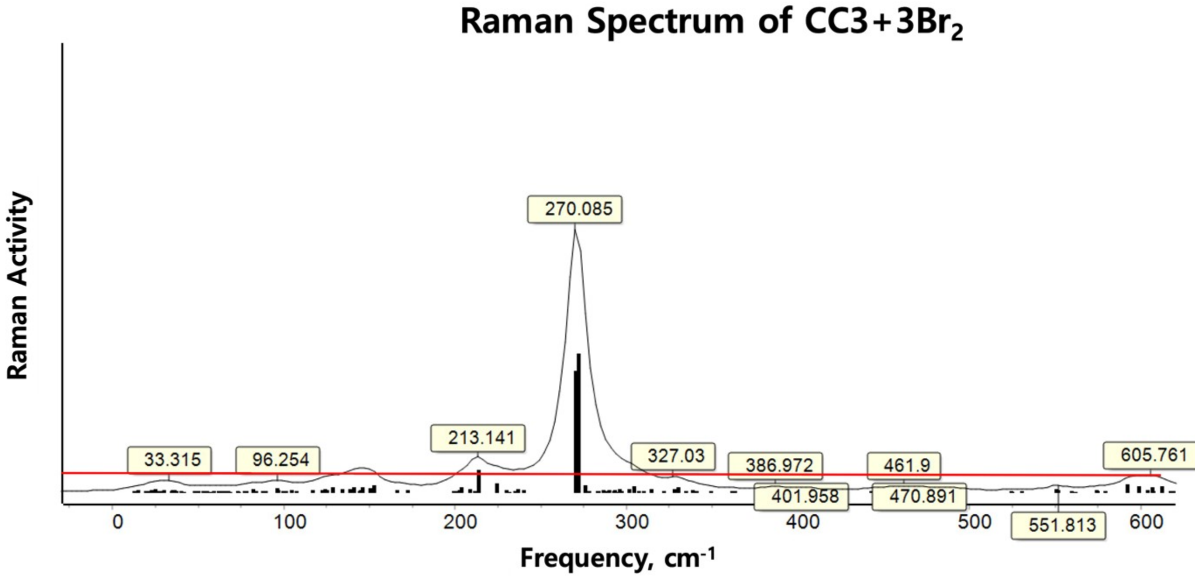

Figure S29. Calculated Raman vibrational spectrum of CC3 with adsorbed 3 molecules of Br$_2$ adsorbed. The red line is the guide to the eyes.

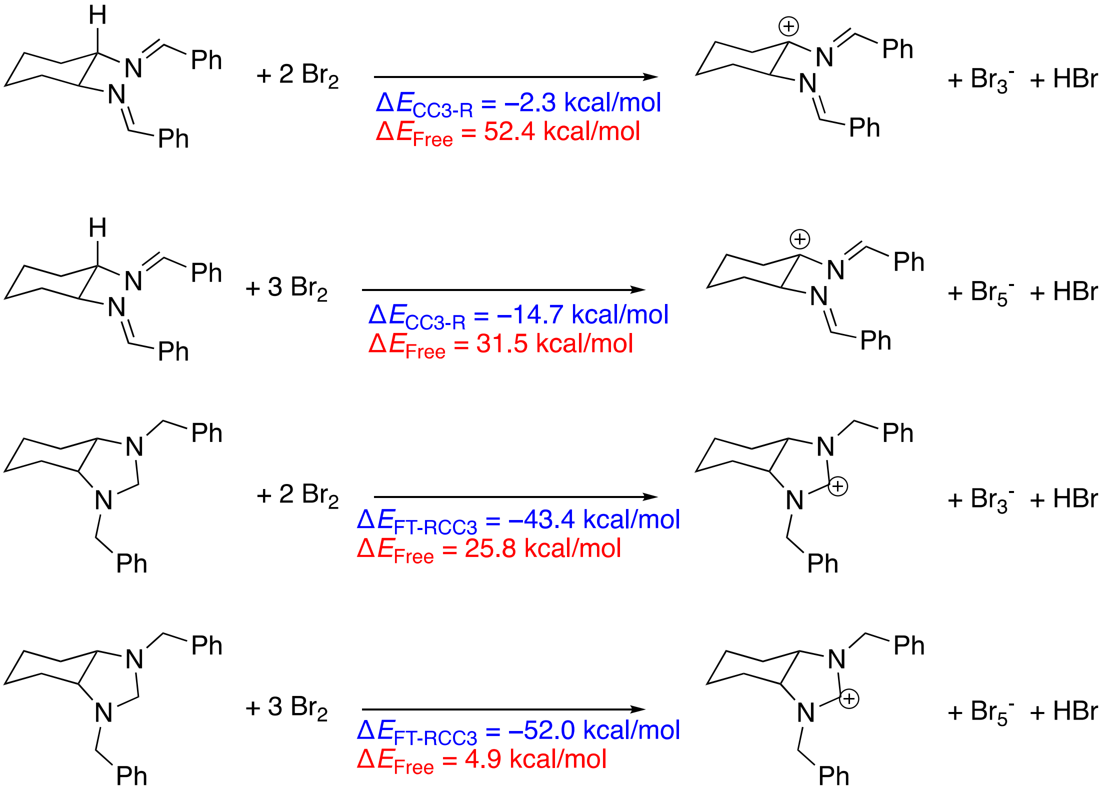

Figure S30. Calculated HBr and carbocation formation reaction energies of POC/Br$_2$ complex and free ligand analogs.

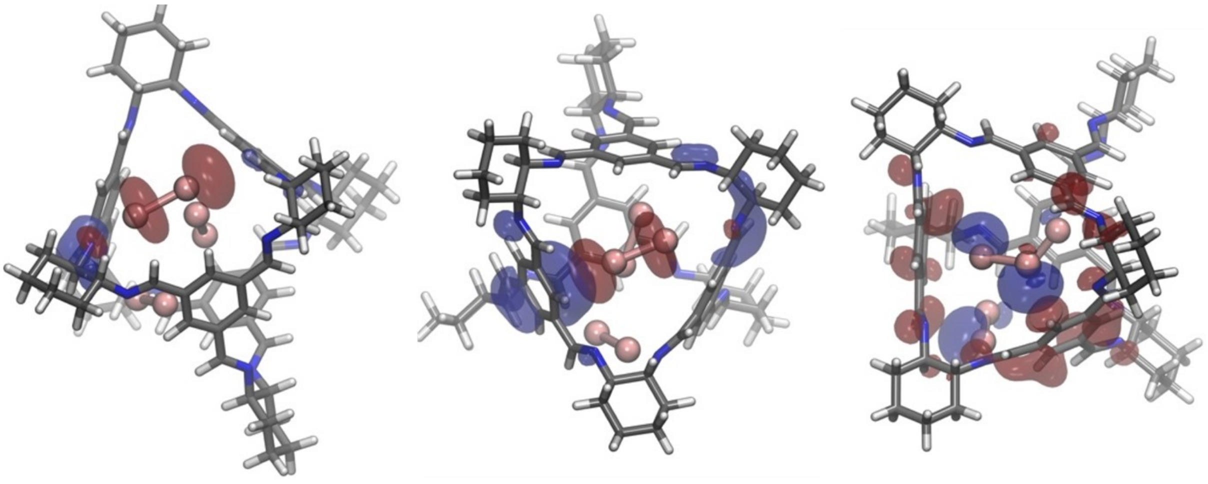

$n_N \rightarrow \sigma^*_{Br\text{-}Br}$
$\Delta E_{int} = -25.1$ kcal/mol

$\pi \rightarrow \sigma^*_{Br\text{-}Br}$
$\Delta E_{int} = -6.6$ kcal/mol

$n_{Br} \rightarrow \pi^*$
$\Delta E_{int} = -8.1$ kcal/mol

Figure S31. Key orbital interactions between CC3-R cage and 3 Br_2 molecules obtained from COVP analysis.

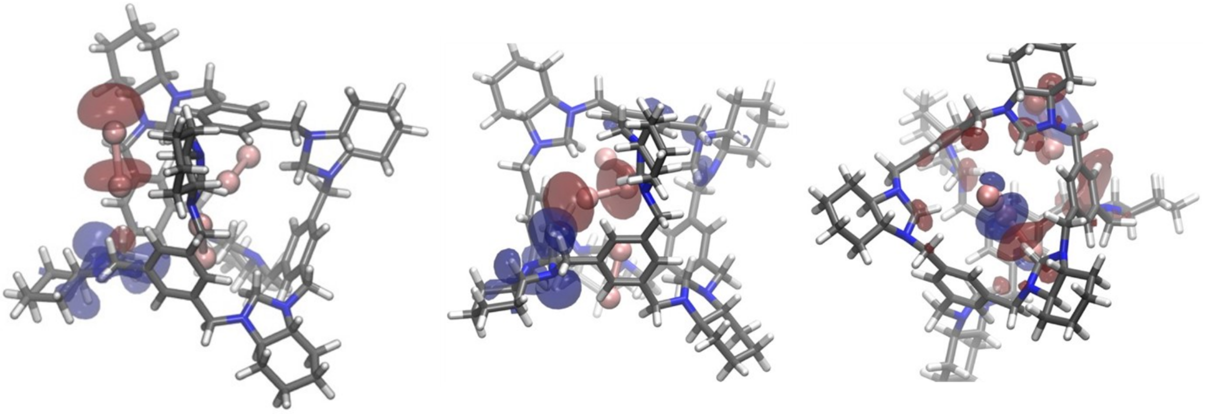

$n_N \rightarrow \sigma^*_{Br\text{-}Br}$
$\Delta E_{int} = -17.0$ kcal/mol

$n_N \rightarrow \sigma^*_{Br\text{-}Br}$
$\Delta E_{int} = -4.7$ kcal/mol

$n_{Br} \rightarrow \sigma^*_{C\text{-}H}$
$\Delta E_{int} = -12.6$ kcal/mol

Figure S32. Key orbital interactions between FT-RCC3 cage and 3 Br_2 molecules obtained from COVP analysis.

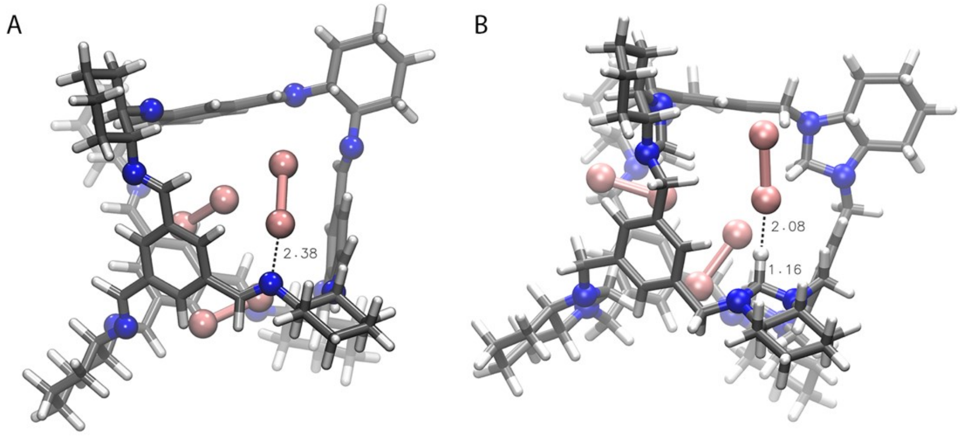

Figure S33. Key secondary interactions in complexes (A) CC3-R@3Br_2 with N−Br distance (2.38 Å) labeled and (B) FT-RCC3@3Br_2 with Br−H (2.08 Å) and C−H (1.16 Å) distance labeled.

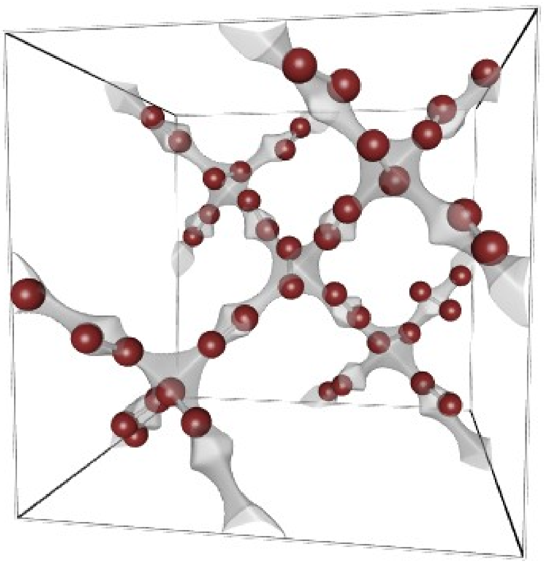

Figure S34. GCMC simulation snapshot of Br_2 adsorbed inside CC3-R cages. Cage atoms were not shown for clarity. Grey colors are the potential energy surface calculated using a Xenon probe from iRASPA software[12].

Tables S1-S9

Table S1. Textural properties and Static Br_2 uptake capacity of various adsorbents.

	S_{BET} ($m^2 \cdot g^{-1}$)	Pore volume ($cm^3 \cdot g^{-1}$)	Static Br_2 vapor uptake ($mmol \cdot g^{-1}$)[a]
CC3-R[b]	404.5	0.158	9.49
FT-RCC3[b]	386.9	0.154	9.71
Co_2Cl_2(BTDD)[13]	-	-	2.207
TCuI[14]	-	-	0.867
TCuBr[14]	-	-	0.300
TCuCl[14]	-	-	0.138
TCuCN[14]	-	-	0.179

[a] The static Br_2 vapor capture experiment was performed at 25 °C during 24 hours.
[b] This work

Table S2. Calculated adsorption rate constant and R-square of CC3-R and FT-RCC3.

		CC3-R	FT-RCC3
Pseudo-first-order	R^2	0.9953	0.9935
	k_1 (min^{-1})	0.0699	0.0810
Pseudo-second-order	R^2	0.9920	0.9905
	k_2 ($g \cdot mmol^{-1} \cdot min^{-1}$)	0.0042	0.0050

Table S3. Elemental composition of Br_2@POCs and thermally treated Br_2@POCs.

Element (%)	Carbon	Nitrogen	Hydrogen	C/N ratio	C/H ratio
Physically mixture of monomers[a]	59.76	11.23	7.139	6.209 (6.000)[b]	0.698 (0.667)[b]
Physically mixture of monomers after thermal treatment[a]	70.30	10.87	6.508	7.545	0.900
Pristine CC3-R	75.04	14.82	7.540	5.907	0.829
Br_2@CC3-R	28.72	6.095	3.557	5.490	0.672
Br_2@CC3-R after thermal treatment	37.73	8.025	4.799	5.485	0.655
Pristine FT-RCC3	75.16	13.84	8.855	6.335	0.707
Br_2@FT-RCC3	25.51	4.689	3.423	6.348	0.621
Br_2@FT-RCC3 after thermal treatment	49.83	9.178	5.455	6.334	0.761

[a] Molar ratio of TFB : CHDA = 2 : 3

[b] Theoretical value of atomic ratio

Table S4. Br/C ratio of Br_2@POCs and thermally treated Br_2@POCs.

	Br_2@CC3-R	Br_2@CC3-R after thermal treatment	Br_2@FT-RCC3	Br_2@FT-RCC3 after thermal treatment
Br/C ratio	0.4607	0.1465	0.2466	0.0457

Table S5. Calculated adsorption energies of Br_n species with CC3-R and FT-RCC3. All reported energies are in kcal/mol. All energies are relative to free CC3-R, FT-RCC3 and Br_2.

	Br_2	2 Br_2	Br_3+HBr	3 Br_2	Br_5+HBr
CC3-R	−16.9	−31.6	−33.9	−47.9	−62.6
FT-RCC3	−18.3	−30.6	−74.0	−43.6	−95.6

Table S6. Decomposition analysis of interaction energies between POCs and bromine clusters. All energies are in kcal/mol.

		$\Delta E_{\mathrm{elstat}}$	$\Delta E_{\mathrm{dispersion}}$	$\Delta E_{\mathrm{pauli}}$	ΔE_{pol}	ΔE_{ct}
CC3	Br_2	−11.8	−17.8	19.0	−0.4	−6.4
	Br_3^-	−84.2	−25.9	45.7	−13.1	−14.5
	Br_4	−53.3	−33.0	82.8	−4.0	−28.1
	Br_5^-	−89.2	−40.4	57.6	−9.9	−16.7
	Br_6	−86.6	−49.7	139.5	−7.8	−49.0
FT-RCC3	Br_2	−17.6	−18.5	26.7	−8.8	−18.7
	Br_3^-	−86.0	−30.1	51.4	−14.4	−18.7
	Br_4	−33.2	−31.1	51.5	−1.4	−14.2
	Br_5^-	−95.6	−44.0	75.5	−11.3	−21.8
	Br_6	−57.3	−48.3	103.4	−2.9	−40.7

Table S7. Benchmark data of the Bromine vibrational frequencies.[15, 16]

	Fundamental (cm^{-1})
Exp. Liquid (gas)	318.6 (323.2)
BLYP	281
BLYP-D4*	282
B3LYP	303
B3LYP-D4*	304
M06-2X-TZVP	332
M06-2X-SVP**	325

* 58 seconds with 48 cores

** 92 seconds with 48 cores

Table S8. LJ parameters for all atoms and molecules used in the GCMC simulation.

Atom Type	ϵ/k_B (K)	σ (Å)
N	38.9492	3.262
C	47.8562	3.472
H	7.6489	2.846
Br_br$_2$	280.39	3.4166

Table S9. Comparison of the saturation loading of Br$_2$ molecules in FT-RCC3 and CC3-R from this work and the work by Khanchi and co-workers[17].

Framework Type	**Saturation Loading (mmol/g)**	**Reference**
CC3-R	2.65	This work
	5.00	Khanchi et al.[17]
FT-RCC3	2.47	This work

References

1 F. Neese, The ORCA program package, *Wiley Interdiscip. Rev. Comput. Mol. Sci.*, 2012, **2**, 73–78.

2 a) A. D. Becke, Density-functional thermochemistry. III. The role of exact exchange, *J. Chem. Phys.*, 1993, **98**, 5648–5652. b) C. Lee, W. Yang, R. G. Parr, Development of the Colle-Salvetti correlation-energy formula into a functional of the electron density, *Phys. Rev. B Condens. Matter*, 1988, **37**, 785–789. c) P. J. Stephens, F. J. Devlin, C. F. Chabalowski, M. J. Frisch, Ab initio calculation of vibrational absorption and circular dichroism spectra using density functional force fields, *J. Phys. Chem.*, 1994, **98**, 11623–11627.

3 a) E. Caldeweyher, C. Bannwarth, S. Grimme, Extension of the D3 dispersion coefficient model, *J. Chem. Phys.*, 2017, **147**, 034112. b) E. Caldeweyher, S. Ehlert, A. Hansen, H. Neugebauer, S. Spicher, C. Bannwarth, S. Grimme, A generally applicable atomic-charge dependent London dispersion correction, *J. Chem. Phys.*, 2019, **150**, 154122.

4 F. Eckert, P. Pulay, H.-J. Werner, Ab initio geometry optimization for large molecules, *J. Comput. Chem.*, 1997, **18**, 1473–1483.

5 P. R. Horn, Y. Mao, M. Head-Gordon, Probing non-covalent interactions with a second generation energy decomposition analysis using absolutely localized molecular orbitals, *Phys. Chem. Chem. Phys.*, 2016, **18**, 23067–23079.

6 Y. Shao, Z. Gan, E. Epifanovsky, A. T. B. Gilbert, M. Wormit, J. Kussmann, A. W. Lange, A. Behn, J. Deng, X. Feng, D. Ghosh, M. Goldey, P. R. Horn, L. D. Jacobson, I. Kaliman, R. Z. Khaliullin, T. Kuś, A. Landau, J. Liu, E. I. Proynov, Y. M. Rhee, R. M. Richard, M. A. Rohrdanz, R. P. Steele, E. J. Sundstrom, H. L. Woodcock, P. M.

Zimmerman, D. Zuev, B. Albrecht, E. Alguire, B. Austin, G. J. O. Beran, Y. A. Bernard, E. Berquist, K. Brandhorst, K. B. Bravaya, S. T. Brown, D. Casanova, C.-M. Chang, Y. Chen, S. H. Chien, K. D. Closser, D. L. Crittenden, M. Diedenhofen, R. A. DiStasio, H. Do, A. D. Dutoi, R. G. Edgar, S. Fatehi, L. Fusti-Molnar, A. Ghysels, A. Golubeva-Zadorozhnaya, J. Gomes, M. W. D. Hanson-Heine, P. H. P. Harbach, A. W. Hauser, E. G. Hohenstein, Z. C. Holden, T.-C. Jagau, H. Ji, B. Kaduk, K. Khistyaev, J. Kim, J. Kim, R. A. King, P. Klunzinger, D. Kosenkov, T. Kowalczyk, C. M. Krauter, K. U. Lao, A. D. Laurent, K. V. Lawler, S. V. Levchenko, C. Y. Lin, F. Liu, E. Livshits, R. C. Lochan, A. Luenser, P. Manohar, S. F. Manzer, S.-P. Mao, N. Mardirossian, A. V. Marenich, S. A. Maurer, N. J. Mayhall, E. Neuscamman, C. M. Oana, R. Olivares-Amaya, D. P. O'Neill, J. A. Parkhill, T. M. Perrine, R. Peverati, A. Prociuk, D. R. Rehn, E. Rosta, N. J. Russ, S. M. Sharada, S. Sharma, D. W. Small, A. Sodt, T. Stein, D. Stück, Y.-C. Su, A. J. W. Thom, T. Tsuchimochi, V. Vanovschi, L. Vogt, O. Vydrov, T. Wang, M. A. Watson, J. Wenzel, A. White, C. F. Williams, J. Yang, S. Yeganeh, S. R. Yost, Z.-Q. You, I. Y. Zhang, X. Zhang, Y. Zhao, B. R. Brooks, G. K. L. Chan, D. M. Chipman, C. J. Cramer, W. A. Goddard, M. S. Gordon, W. J. Hehre, A. Klamt, H. F. Schaefer, M. W. Schmidt, C. D. Sherrill, D. G. Truhlar, A. Warshel, X. Xu, A. Aspuru-Guzik, R. Baer, A. T. Bell, N. A. Besley, J.-D. Chai, A. Dreuw, B. D. Dunietz, T. R. Furlani, S. R. Gwaltney, C.-P. Hsu, Y. Jung, J. Kong, D. S. Lambrecht, W. Liang, C. Ochsenfeld, V. A. Rassolov, L. V. Slipchenko, J. E. Subotnik, T. Van Voorhis, J. M. Herbert, A. I. Krylov, P. M. W. Gill, M. Head-Gordon, Advances in molecular quantum chemistry contained in the Q-Chem 4 program package, *Mol. Phys.*, 2015, **113**, 184–215.

7 R. Z. Khaliullin, A. T. Bell, M. Head-Gordon, Analysis of charge transfer effects in molecular complexes based on absolutely localized molecular orbitals, *J. Chem. Phys.*, 2008, **128**, 184112.

8 E. Caldeweyher, J.-M. Mewes, S. Ehlert, S. Grimme, Extension and evaluation of the D4 London-dispersion model for periodic systems, *Phys. Chem. Chem. Phys.*, 2020, **22**, 8499–8512.

9 Rappé, A. K, Casewit, C. J, Colwell, K, Goddard Iii, W, Skiff, W, UFF, a full periodic table force field for molecular mechanics and molecular dynamics simulations, *J. Am. Chem. Soc.*, 1992, **114**, 10024-10035.

10 Stöbener, K, Klein, P, Horsch, M, Küfer, K, Hasse, H, Parametrization of two-center Lennard-Jones plus point-quadrupole force field models by multicriteria optimization, *Fluid Phase Equilibr*, 2016, **411**, 33-42.

11 Dubbeldam, D, Calero, S, Ellis, D. E, Snurr, R. Q, RASPA: molecular simulation software for adsorption and diffusion in flexible nanoporous materials, *Mol Simulat*, 2016, **42**, 81-101.

12 Dubbeldam, D, Calero, S, Vlugt, T. J. H, iRASPA: GPU-accelerated visualization software for materials scientists, *Mol Simulat*, 2018, 44, 653-676.

13 Y. Tulchinsky, C. H. Hendon, K. A. Lomachenko, E. Borfecchia, B. C. Melot, M. R. Hudson, J. D. Tarver, M. D. Korzyński, A. W. Stubbs, J. J. Kagan, C. Lamberti, C. M. Brown, M. Dincă, Reversible Capture and Release of Cl_2 and Br_2 with a Redox-Active Metal-Organic Framework, *J. Am. Chem. Soc.*, 2017, **139**, 5992–5997.

14 S.-L. Zheng, Y. He, X.-K. Qiu, Y.-H. Zhong, L.-H. Chung, W.-M. Liao, J. He, Synthesis, structures and Br_2 uptake of Cu(I)-bipyrazole frameworks, *J. Solid State Chem.*, 2021, **302**, 122458.

15 E. T. Branigan, M. N. van Staveren, V. A. Apkarian, Solidlike coherent vibronic dynamics in a room temperature liquid: Resonant Raman and absorption spectroscopy of liquid bromine, *J. Chem. Phys.*, 2010, **132**, 044503.

16 K.P. Huber, G. Herzberg, Constants of Diatomic Molecules (data prepared by J.W. Gallagher, R.D. Johnson, III) in NIST Chemistry WebBook, NIST Standard Reference Database Number 69, edited by P.J. Linstrom, W.G. Mallard, July 2001, National Institute of Standards and Technology, Gaithersburg MD, 20899 (http://webbook.nist.gov).

17 Ghalami, Z, Ghoulipour, V, Khanchi, A. R. Adsorption and sequential thermal release of F_2, Cl_2, and Br_2 molecules by a porous organic cage material (CC3-R): Molecular dynamics and grand-canonical Monte Carlo simulations, *J Comput Chem*, 2020, **41**, 949-957.